Research Article | Vol. 29, No. 9 / 26 April 2021 / Optics Express 13960

Optics EXPRESS

Hybrid evaporative cooling of ^{133}Cs atoms to Bose-Einstein condensation

YUNFEI WANG,[1] YUQING LI,[1,2,5] JIZHOU WU,[1,2] WENLIANG LIU,[1,2] JIAZHONG HU,[3,4] JIE MA,[1,2,6] LIANTUAN XIAO,[1,2] AND SUOTANG JIA[1,2]

[1] *State Key Laboratory of Quantum Optics and Quantum Optics Devices, Institute of Laser Spectroscopy, Shanxi University, Taiyuan 030006, China*
[2] *Collaborative Innovation Center of Extreme Optics, Shanxi University, Taiyuan, Shanxi 030006, China*
[3] *Department of Physics and State Key Laboratory of Low Dimensional Quantum Physics, Tsinghua University, Beijing 100084, China*
[4] *Frontier Science Center for Quantum Information, Beijing 100084, China*
[5] *lyqing.2006@163.com*
[6] *mj@sxu.edu.cn*

Abstract: The Bose-Einstein condensation (BEC) of ^{133}Cs atoms offers an appealing platform for studying the many-body physics of interacting Bose quantum gases, owing to the rich Feshbach resonances that can be readily achieved in the low magnetic field region. However, it is notoriously difficult to cool ^{133}Cs atoms to their quantum degeneracy. Here we report a hybrid evaporative cooling of ^{133}Cs atoms to BEC. Our approach relies on a combination of the magnetically tunable evaporation with the optical evaporation of atoms in a magnetically levitated optical dipole trap overlapping with a dimple trap. The magnetic field gradient is reduced for the magnetically tunable evaporation. The subsequent optical evaporation is performed by lowering the depth of the dimple trap. We study the dependence of the peak phase space density (PSD) and temperature on the number of atoms during the evaporation process, as well as how the PSD and atom number vary with the trap depth. The results are in excellent agreement with the equation model for evaporative cooling.

1. Introduction

The quantum degenerate atomic gas provides a versatile platform with unprecedented controllability for the fundamental studies of many-body physics [1]. In particular, in ultracold atom experiments the scattering length characterizing the atomic interactions can be flexibly tuned using Feshbach resonances [2]. This has paved the way for the studies such as the BEC-BCS crossover [3,4] and the thermodynamic properties of degenerate Fermi gases in the unitary limit [5–7]. The properties of Bose gases can also be modified by Feshbach resonances, and the universal scaling laws exhibited by strongly interacting Bose gases have received considerable interests [8–10]. In this context, a unique advantage of ^{133}Cs atoms over many other alkali-metal atoms is their rich Feshbach resonances [11]. The smooth variation of scattering length in the low magnetic field region centred about - 11.7 G allows the interatomic interactions to be monotonously and gently tuned in a large range [12,13]. For example, the s-wave scattering length varies from ~ -2500 to 1400 a_0 (Bohr radius) when the magnetic field is tuned from 0 to 100 G [11]. Near a low magnetic field of $\sim$ 17 G, ^{133}Cs atoms can be used to produce the matter-wave solitons [14–16] and the modulation of scattering length at low magnetic field can form the collective emission of matter-wave jets and atomic density patterns [17,18]. Moreover, ^{133}Cs atoms have several narrow Feshbach resonances, which are important for the formation of ultracold ground-state molecules [19–21].

#419854 https://doi.org/10.1364/OE.419854
Journal © 2021 Received 19 Jan 2021; revised 11 Apr 2021; accepted 14 Apr 2021; published 22 Apr 2021

Optics EXPRESS

While ^{133}Cs atoms offer many adavantages over other alkali metal atoms due to their highly tunable interaction, it is notoriously difficult to cool them to quantum degeneracy. As mentioned in Ref. [22], such a difficulty is associated with the large two- and three-body inelastic collisions [23–27]. To effectively suppress the endothermic inelastic two-body collisions, three-dimensional (3D) degenerate Raman sideband cooling (dRSC) had been used to prepare a low temperature atomic sample in the $F = 3$, $m_F = 3$ state [28–30], thus enabling the evaporation of optically trapped atoms towards the BEC. Furthermore, a broad Feshbach resonance must be used to tune the scattering length from the negative to positive in order to avoid the collapse of condensate. ^{133}Cs BEC was first achieved in a magnetically levitated dimple trap [31,32]. Since then, there have been significant progress in the studies of the few-body physics [27], the ultracold ground-state molecules [19,20] and the strongly correlated quantum gases in optical lattices [12,13,33] in the groups of Prof. Nägerl and Prof. Grimm. Accelerated evaporative cooling of ^{133}Cs atoms was realized by using the magnetic field gradient to tilt the dipole trap [34]. Efficient sympathetic cooling with ^{87}Rb atoms was also used to obtain the ^{133}Cs BEC [35]. More recently, dRSC was used to achieve a quantum gas of ^{133}Cs atoms by the direct laser cooling with a small atom number of ~ 300 [22].

In this paper, we present the hybrid evaporative cooling approach for producing ^{133}Cs BEC. The cold atoms cooled by 3D dRSC are loaded into a magnetically levitated dipole trap. We moreover add a tight dimple trap to improve the trapping frequency and increase the atomic density [14,31,36–38]. The hybrid evaporative cooling consists of two stages. The initial evaporation is implemented by reducing the magnetic field gradient to tilt the trap. In the second stage, an optical evaporative cooling is performed in the tilted dimple trap by reducing the powers of two dimple trap laser beams. We study the dependence of the peak phase space density (PSD) and temperature on the number of atoms during the hybrid evaporation. The variations of the atom number and PSD with the trap depth are investigated. The equation model based on the scaling laws for the evaporative cooling is used to explain the experimental results.

2. Hybrid evaporative cooling to Bose-Einstein condensation

Two horizontally crossed 1064-nm laser beams at an angle of 90° are used to form the crossed dipole trap for loading the atoms cooled by 3D dRSC. The two dipole trap laser beams almost have the same beam waist of ~ 300 μm. The initial trapping frequencies are $\omega_{x,y,z} = 2\pi \times (18, 18, 25)$ Hz near the bottom of the trap. Because the large gravity of ^{133}Cs atoms induces a large destructive potential in the vertical direction, the atoms have to be loaded into a magnetically levitated dipole trap [14,31,34]. The uniform magnetic field is firstly kept at $B = 75$ G for 300 ms and then reduced to 40 G in 200 ms. The corresponding s-wave scattering length changes from $a = 1228\ a_0$ to $793\ a_0$. After thermalization within 0.5 s in the magnetically levitated dipole trap, there are 9.5×10^6 atoms at a temperature of $T = 2.5$ μK. The atomic density and PSD are approximately 6×10^{11} cm^{-3} and 5×10^{-4}, respectively. To increase the atomic density and PSD, we add a tight dimple trap, which is formed by two 1064-nm laser beams with almost the same radius of 58 μm. The angle between the dimple laser and the dipole trap laser is about 12°. The powers of two dimple lasers are linearly ramped to 100 mW within 500 ms. The trapping frequencies on the bottom of the combined potential are increased to $\omega_{x,y,z} = 2\pi \times (98, 98, 139)$ Hz. To minimize the three-body loss of atoms during the loading of dimple trap, the uniform magnetic field is fixed at $B = 40$ G for 250 ms before being reduced to 26.4 G in 250 ms, the corresponding scattering length is reduced to $435\ a_0$.

After the loading of dimple trap, the number of atoms reduces to $N = 2.6 \times 10^6$ with a temperature of $T = 3.4$ μK; however, the peak atomic density increases to $n = 1.8 \times 10^{13}$ cm^{-3} and the PSD is locally increased by a factor of 20. Afterwards, we perform the hybrid evaporative cooling of atoms. Figure 1(a) shows the time sequence for the hybrid evaporative cooling, with its two stages shown in Figs.1 (b) and (c), respectively. Initial evaporation is performed by tilting

Optics EXPRESS

the trap in the vertical direction. The magnetic field gradient is linearly reduced from $\partial B/\partial z$ = 31.3 G/cm to 20 G/cm in 1.5 s at the uniform magnetic field of 26.4 G. Subsequently, the magnetic field gradient and uniform magnetic field are reduced to 10 G/cm and 23 G in 1 s and then to 0 and 21.9 G in another 1 s, respectively. The corresponding scattering length is reduced to 304 a_0 and then to 257 a_0. The powers of the two dipole laser beams are reduced to 0 in the last 1 s of the initial evaporation. There are $N = 2.2 \times 10^5$ atoms in the dimple trap at a temperature of $T = 0.38$ μK and the PSD is about 0.41.

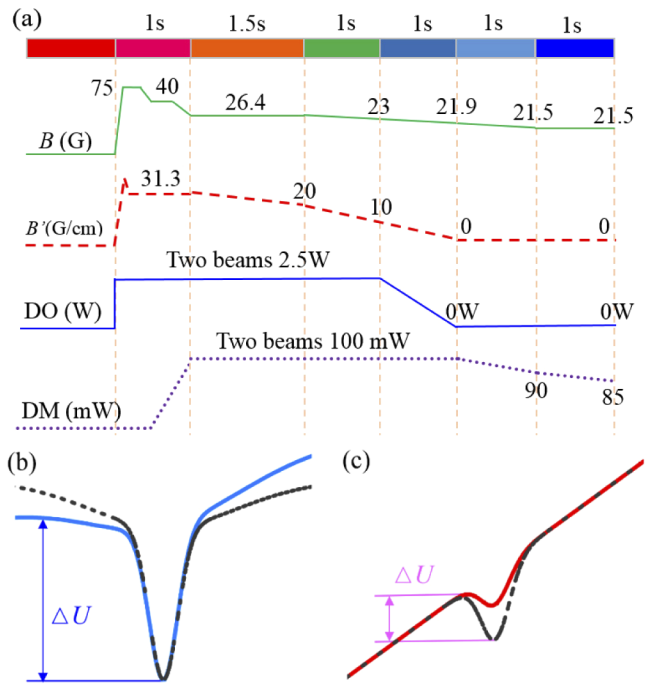

Fig. 1. (a) Time sequence of hybrid evaporative cooling. A tight dimple trap is added to increase the PSD of atoms in the magnetically levitated dipole trap. The initial evaporation is performed by linearly reducing magnetic field gradient. The optical evaporation is subsequently implemented by reducing the powers of two dimple trap lasers. During the entire evaporation, a uniform magnetic field is used to continuously tune the atomic *s*-wave scattering length, in order to reduce the atom loss induced by the three-body recombination. DO, dipole trap; DM, dimple trap. (b) Schematic of the initial evaporation. The trap is tilted by reducing the magnetic field gradient for reducing the trap depth in the vertical direction. (c) After switching off the magnetic field gradient and dipole trap, the optical evaporative cooling is implemented by reducing the powers of two dimple trap laser beams for reducing the depth of the tilted dimple trap.

Optical evaporative cooling is implemented by reducing the depth of dimple trap, and the powers of the two dimple trap laser beams are reduced synchronously. The uniform magnetic field is continuously tuned to minimize the three-body loss of atoms. As shown in Fig. 1(a), the power of the dimple laser beam is reduced from 100 mW to 90 mW in 1 s. The uniform magnetic field is also reduced from 21.9 G to 21.5 G, and the scattering length changes from 257 a_0 to 238 a_0. Here we obtain 1.15×10^5 atoms at a temperature of $T = 157$ nK, and the PSD is about 2.1. When the power of the dimple laser beam is reduced to 85 mW, a nearly pure BEC is achieved with 7×10^4 atoms at the temperature of $T = 70$ nK. The PSD is estimated as 6 when we consider the condensation in the Thomas-Fermi regime. Figure 2 shows three

Optics EXPRESS

absorption images after the 18 ms time-of-flight (TOF) at zero scattering length near 17 G, which correspond to the power of 100, 90 and 85 mW of the dimple trap laser, respectively. A bimodal distribution of optical density is clearly demonstrated as the optical evaporation is implemented after the initial evaporation.

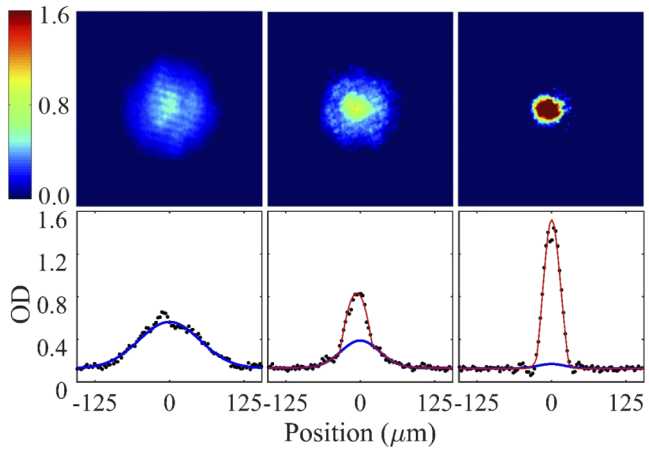

Fig. 2. Condensation of ^{133}Cs atoms. Absorption images (top) taken after 18 ms time-of-flight at zero scattering length near 17 G. From left to right, the power of the dimple trap laser is 100, 90, and 85 mW, the corresponding temperature is 380, 157 and 70 nK. Single-line optical density (OD) profiles (bottom) are taken from the top images. The blue curve is a Gaussian fit for the distribution of OD, the red curve represents a fit with the bimodal distribution.

3. Dependence of PSD and temperature on the atom number

To evaluate the efficiency of our hybrid evaporative cooling, we plot in Fig. 3 the PSD and temperature during the evaporation as a function of the atom number. The temperatures of the atoms at various evaporative steps are extracted from the absorption images taken at different times of flight near 17 G, where the scattering length is zero. The PSD is calculated as $D = n\lambda_{dB}^3$, where $n = N\omega_x\omega_y\omega_z(m\lambda_{dB}/h)^3$ is the peak atomic density, $\lambda_{dB} = h(2\pi mk_BT)^{-1/2}$ is the thermal de Broglie wavelength, h is the Planck constant, and k_B is the Boltzmann constant [39]. The trapping frequencies during the evaporation are deduced from the calibrated properties of the trap. We find that peak atomic density n is located between 1.8×10^{13} and 3.9×10^{13} cm^{-3} during the entire evaporation.

The mean evaporation efficiency is calculated as $\overline{\gamma}$ = -ln(D/D_0)/ln(N/N_0) = 3.14 ± 0.14, where D_0 and N_0 are the PSD and atom number after the loading of dimple trap. Based on the calculated $\overline{\gamma}$, we analyze the dependence of PSD on the atom number, and the numeric calculation agrees well with the experimental data, as shown in Fig. 3. Following the analyses for the evaporative cooling, the temperature shows a power-law dependence on the atom number as $T \propto N^{\alpha}$. Here α parameterizes the cooling efficiency by removing atoms, and it is defined as

$$\alpha = \frac{N}{T}\frac{dT}{dN} = \frac{\eta' - 3}{3 - 3\nu}, \tag{1}$$

where $\eta' = \eta + (\eta - 5)/(\eta - 4)$. In the evaporation process, the mean truncation parameter is calculated as $\eta = \langle U/k_BT\rangle = 6.2$, and U is the depth of trapping potential in the vertical direction. The mean trapping frequency varies with the trap depth as $\overline{\omega} \propto U^{\nu}$, where $\nu = 0.079$ is obtained by fitting the variation of $\overline{\omega}$ with U in the hybrid evaporation. By substituting the calculated η

Optics EXPRESS

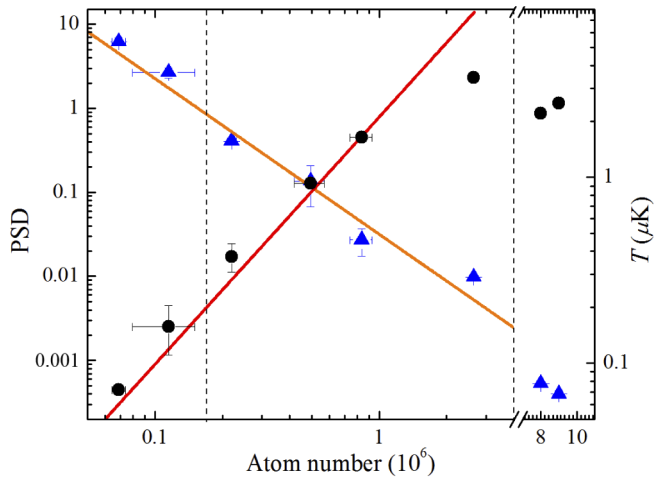

Fig. 3. PSD (blue triangles) and temperature (black dots) during the evaporative cooling as a function of the atom number. The data between two vertical dashed lines are taken from the initial evaporation process. The data on the left side of the left vertical dashed line are taken from the optical evaporation. The orange line shows the numerical calculation with a mean evaporative efficiency of $\overline{\gamma} = 3.14 \pm 0.14$. The red line shows a power-law fit for the dependence of temperature on the atom number with $\alpha = 1.35$.

and the fitted ν into Eq. (1), α is derived as 1.35. Using the power-law dependence of temperature on the atom number, a good fit for the data is obtained, as shown in Fig. 3.

4. Variations of the atom number and PSD with trap depth

Figure 4 shows the variations of the atom number and PSD during the hybrid evaporative cooling with the trap depth in the vertical direction. According to the derived scaling laws for evaporative cooling in time-dependent optical traps [40], the number of atoms varies with trap depth as

$$\frac{N}{N_i} = (\frac{U}{U_i})^{3/[2(\eta'-3)]}, \tag{2}$$

where i denotes the initial condition at the beginning of the hybrid evaporation, $N = N(t)$ and $U = U(t)$. When Eq. (2) is used to fit the experimental data, a good fitting is obtained for $\eta = 6.16$, which is consistent with our calculation. For ^{133}Cs atoms, the destructive potential induced by the large gravity has an impact on the trap depth in the vertical direction when the optical trap becomes weak during the final evaporative steps. Compared to other experiments with a larger η, our optical evaporation by lowering the power of the dimple laser significantly decreases the vertical trapping potential of the tilted dimple trap as compared to the horizontal trapping potential.

Regarding the variation of PSD with trap depth, theoretical analysis shows that the PSD scales with trap depth as

$$\frac{D}{D_i} = (\frac{U_i}{U})^{3(\eta'-4)/[2(\eta'-3)]}, \tag{3}$$

where D_i is the initial PSD and $D = D(t)$. Equation (3) is used to obtain a good fit for the experimental data, as shown in Fig. 4.

Optics EXPRESS

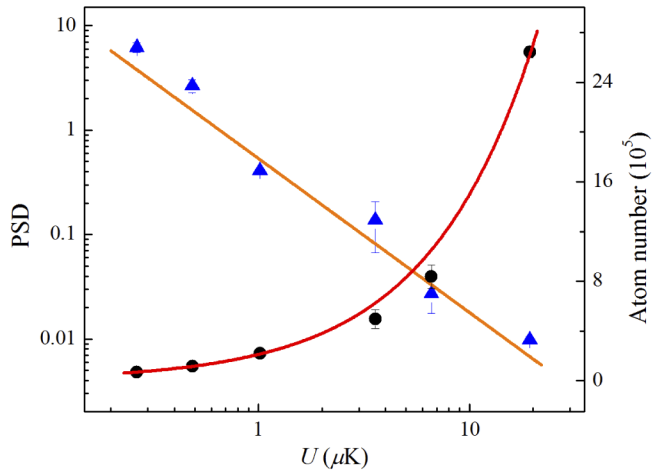

Fig. 4. Variations of the atom number (black circles) and PSD (blue triangles) during the evaporative cooling as a function of trap depth. The solid curves are the fitting curves based on the scaling laws, which contain the theoretical dependence of the atom number and PSD on the trap depth.

5. Discussion

Condensation of ^{133}Cs atoms was firstly produced by the optical evaporative cooling in the magnetically levitated optical trap [31]. Our hybrid evaporative cooling is different from the optimized optical evaporation [32] in several aspects. First, the geometrical configuration and experimental parameters of optical traps are different. Second, the hybrid evaporative cooling allows for an effective combination of the magnetically tunable evaporation and the optical evaporation, the latter is implemented in the tilted dimple trap in our setup. Third, the hybrid evaporative cooling allows for a fast evaporation, taking ~ 6.5 s to achieve BEC after the loading of Magneto-optical trap (MOT). We also find that the time is reduced to 6.8 s to obtain the BEC after the loading of MOT in the new apparatus in Nägerl's group [41].

A faster evaporative cooling was demonstrated by using the trap-tilting evaporation [34]. In comparison, the geometrical configuration and experimental parameters of the dipole trap in our setup are very similar to the ones used in the trap-tilting evaporation. The trapping frequencies of the magnetically levitated dipole trap are smaller than the trapping frequencies in Ref. [34], although the slightly higher powers are used for two dipole trap laser beams in our setup. Thus, the dimple trap is added for increasing the density of atoms in the magnetically levitated dipole trap. In our hybrid evaporative cooling, the scheme for the initial evaporation is same as the trap-tilting evaporation, except for the utility of a reduced magnetic field gradient. However, the subsequent optical evaporation allows for the achievement of ^{133}Cs BEC in a tilted dimple trap. We also note that a light sheet with the elliptical laser beam was used in Chin's group to support the atoms against gravity and prepare Cs BEC in the purely optical trap [42].

6. Conclusion

We have demonstrated a hybrid evaporative cooling approach for producing ^{133}Cs BEC, which combines the magnetically tunable evaporation of atoms by tilting the optical trap and the optical evaporation in a dimple trap. The uniform magnetic field is continuously tuned to alter the atomic interaction and reduce the three-body loss of atoms. The nearly pure Cs atom condensate is obtained in a tilted dimple trap. The dependence of the PSD and temperature during evaporation on the number of atoms are studied, and the scaling laws for evaporative cooling are used to

Optics EXPRESS

obtain good explanations for the experimental results. The variations of the atom number and PSD with the trap depth are in excellent agreement with the equation model for evaporative cooling.

Funding. National Key Research and Development Program of China (2017YFA0304203); National Natural Science Foundation of China (61675121, 61705123, 61722507); Program for Changjiang Scholars and Innovative Research Team in University (IRT17R70); Open Research Fund Program of the State Key Laboratory of Low-Dimensional Quantum Physics; Applied Basic Research Project of Shanxi Province (201901D211191); Collaborative grant by the Russian Foundation for Basic Research and NSF of China (20-53-53025, 62011530047).

Acknowledgments. We acknowledge the helpful suggestions on the design of the experimental apparatus from Professor Cheng Chin and the help of Professor Ying Hu on the revision of manuscript.

Disclosures. The authors declare no conflicts of interest.

References

1. I. Bloch, J. Dalibard, and W. Zwerger, "Many-body physics with ultracold gases," Rev. Mod. Phys. **80**(3), 885–964 (2008).
2. C. Chin, R. Grimm, P. Julienne, and E. Tiesinga, "Feshbach resonances in ultracold gases," Rev. Mod. Phys. **82**(2), 1225–1286 (2010).
3. T. Bourdel, L. Khaykovich, J. Cubizolles, J. Zhang, F. Chevy, M. Teichmann, L. Tarruell, S. J. J. M. F. Kokkelmans, and C. Salomon, "Experimental Study of the BEC-BCS Crossover Region in Lithium 6," Phys. Rev. Lett. **93**(5), 050401 (2004).
4. M. W. Zwierlein, J. R. Abo-Shaeer, A. Schirotzek, C. H. Schunck, and W. Ketterle, "Vortices and superfluidity in a strongly interacting Fermi gas," Nature **435**(7045), 1047–1051 (2005).
5. M. J. H. Ku, A. T. Sommer, L. W. Cheuk, and M. W. Zwierlein, "Revealing the Superfluid Lambda Transition in the Universal Thermodynamics of a Unitary Fermi Gas," Science **335**(6068), 563–567 (2012).
6. M. K. Tey, L. A. Sidorenkov, E. R. S. Guajardo, R. Grimm, M. J. H. Ku, M. W. Zwierlein, Y.-H. Hou, L. Pitaevskii, and S. Stringari, "Collective Modes in a Unitary Fermi Gas across the Superfluid Phase Transition," Phys. Rev. Lett. **110**(5), 055303 (2013).
7. S. J. Deng, Z. -Y Shi, P. P. Diao, Q. L. Yu, H. Zhai, R. Qi, and H. B. Wu, "Observation of the Efimovian expansion in scale-invariant Fermi gases," Science **353**(6297), 371–374 (2016).
8. P. Makotyn, C. E. Klauss, D. L. Goldberger, E. A. Cornell, and D. S. Jin, "Universal dynamics of a degenerate unitary Bose gas," Nat. Phys. **10**(2), 116–119 (2014).
9. F. Chevy and C. Salomon, "Strongly correlated Bose gases," J. Phys. B **49**(19), 192001 (2016).
10. C. Eigen, J. A. P. Glidden, R. Lopes, E. A. Cornell, R. P. Smith, and Z. Hadzibabic, "Universal prethermal dynamics of Bose gases quenched to unitarity," Nature **563**(7730), 221–224 (2018).
11. C. Chin, V. Vuletić, A. J. Kerman, S. Chu, E. Tiesinga, P. J. Leo, and C. J. Williams, "Precision Feshbach spectroscopy of ultracold Cs2," Phys. Rev. A **70**(3), 032701 (2004).
12. E. Haller, M. Gustavsson, M. J. Mark, J. G. Danzl, R. Hart, G. Pupillo, and H.-C. Nägerl, "Realization of an Excited, Strongly Correlated Quantum Gas Phase," Science **325**(5945), 1224–1227 (2009).
13. E. Haller, M. Rabie, M. J. Mark, J. G. Danzl, R. Hart, K. Lauber, G. Pupillo, and H.-C. Nägerl, "Three-Body Correlation Functions and Recombination Rates for Bosons in Three Dimensions and One Dimension," Phys. Rev. Lett. **107**(23), 230404 (2011).
14. T. Mežnaršič, T. Arh, J. Brence, J. Pišljar, K. Gosar, Ž. Gosar, R. Žitko, E. Zupanič, and P. Jeglič, "Cesium bright matter-wave solitons and soliton trains," Phys. Rev. A **99**(3), 033625 (2019).
15. A. D. Carli, C. D. Colquhoun, G. Henderson, S. Flannigan, G.-L. Oppo, A. J. Daley, S. Kuhr, and E. Haller, "Excitation Modes of Bright Matter-Wave Solitons," Phys. Rev. Lett. **123**(12), 123602 (2019).
16. C.-A. Chen and C.-L. Hung, "Observation of universal quench dynamics and Townes soliton formation from modulational instability in two-dimensional Bose gases," Phys. Rev. Lett. **125**(25), 250401 (2020).
17. L. W. Clark, A. Gaj, L. Feng, and C. Chin, "Collective emission of matter-wave jets from driven Bose-Einstein condensates," Nature **551**(7680), 356–359 (2017).
18. Z. D. Zhang, K.-X. Yao, L. Feng, J. Z. Hu, and C. Chin, "Pattern formation in a driven Bose–Einstein condensate," Nat. Phys. **16**(6), 652–656 (2020).
19. J. Herbig, T. Kraemer, M. Mark, T. Weber, C. Chin, H.-C. Nägerl, and R. Grimm, "Preparation of a Pure Molecular Quantum Gas," Science **301**(5639), 1510–1513 (2003).
20. J. G. Danzl, M. J. Mark, E. Haller, M. Gustavsson, R. Hart, J. Aldegunde, J. M. Hutson, and H.-C. Nägerl, "An ultracold high-density sample of rovibronic ground-state molecules in an optical lattice," Nat. Phys. **6**(4), 265–270 (2010).
21. T. Köhler, K. Góral, and P. S. Julienne, "Production of cold molecules via magnetically tunable Feshbach resonances," Rev. Mod. Phys. **78**(4), 1311–1361 (2006).
22. P. Solano, Y. H. Duan, Y.-T. Chen, A. Rudelis, C. Chin, and V. Vuletić, "Strongly Correlated Quantum Gas Prepared by Direct Laser Cooling," Phys. Rev. Lett. **123**(17), 173401 (2019).

Optics EXPRESS

23. P. J. Leo, E. Tiesinga, P. S. Julienne, D. K. Walter, S. Kadlecek, and T. G. Walker, "Elastic and Inelastic Collisions of Cold Spin-Polarized ^{1}33Cs Atoms," Phys. Rev. Lett. **81**(7), 1389–1392 (1998).
24. D. Guéry-Odelin, J. Söding, P. Desbiolles, and J. Dalibard, "Strong evaporative cooling of a trapped cesium gas," Opt. Express **2**(8), 323 (1998).
25. P. J. Leo, C. J. Williams, and P. S. Julienne, "Collision Properties of Ultracold ^{1}33Cs Atoms," Phys. Rev. Lett. **85**(13), 2721–2724 (2000).
26. C. Chin, V. Vuletić, A. J. Kerman, and S. Chu, "High Resolution Feshbach Spectroscopy of Cesium," Phys. Rev. Lett. **85**(13), 2717–2720 (2000).
27. T. Kraemer, M. Mark, P. Waldburger, J. G. Danzl, C. Chin, B. Engeser, A. D. Lange, K. Pilch, A. Jaakkola, H.-C. Nägerl, and R. Grimm, "Evidence for Efimov quantum states in an ultracold gas of caesium atoms," Nature **440**(7082), 315–318 (2006).
28. A. J. Kerman, V. Vuletić, C. Chin, and S. Chu, "Beyond Optical Molasses: 3D Raman Sideband Cooling of Atomic Cesium to High Phase-Space Density," Phys. Rev. Lett. **84**(3), 439–442 (2000).
29. D.-J. Han, S. Wolf, S. Oliver, C. McCormick, M. T. DePue, and D. S. Weiss, "3D Raman Sideband Cooling of Cesium Atoms at High Density," Phys. Rev. Lett. **85**(4), 724–727 (2000).
30. P. Treutlein, K. Y. Chung, and S. Chu, "High-brightness atom source for atomic fountains," Phys. Rev. A **63**(5), 051401 (2001).
31. T. Weber, J. Herbig, M. Mark, H.-C. Nägerl, and R. Grimm, "Bose-Einstein condensation of cesium," Science **299**(5604), 232–235 (2003).
32. T. Kraemer, J. Herbig, M. Mark, T. Weber, C. Chin, H.-C. Nägerl, and R. Grimm, "Optimized production of a cesium Bose-Einstein condensate," Appl. Phys. B **79**(8), 1013–1019 (2004).
33. F. Meinert, M. J. Mark, E. Kirilov, K. Lauber, P. Weinmann, M. Gräbner, A. J. Daley, and H.-C. Nägerl, "Observation of many-body dynamics in long-range tunneling after a quantum quench," Science **344**(6189), 1259–1262 (2014).
34. C.-L. Hung, X. B. Zhang, N. Gemelke, and C. Chin, "Accelerating evaporative cooling of atoms into Bose-Einstein condensation in optical traps," Phys. Rev. A **78**(1), 011604 (2008).
35. D. J. McCarron, H. W. Cho, D. L. Jenkin, M. P. Köppinger, and S. L. Cornish, "Dual-species Bose-Einstein condensate of Rb87 and Cs133," Phys. Rev. A **84**(1), 011603 (2011).
36. P. W. H. Pinkse, A. Mosk, M. Weidemüller, M. W. Reynolds, T. W. Hijmans, and J. T. M. Walraven, "Adiabatically Changing the Phase-Space Density of a Trapped Bose Gas," Phys. Rev. Lett. **78**(6), 990–993 (1997).
37. C.-Y. Huang, C.-C. Chen, L.-A. Sun, G.-B. Liao, K.-S. Wu, Y.-J. Lin, and M.-S. Chang, "A simple recipe for rapid all-optical formation of spinor Bose-Einstein condensates," J. Phys. B **50**(15), 155302 (2017).
38. D. Z Xie, D. Y. Wang, W. Gou, W. H. Bu, and B. Yan, "Fast production of rubidium Bose-Einstein condensate in a dimple trap," J. Opt. Soc. Am. B **35**(3), 500 (2018).
39. A. J. Olson, R. J. Niffenegger, and Y. P. Chen, "Optimizing the efficiency of evaporative cooling in optical dipole traps," Phys. Rev. A **87**(5), 053613 (2013).
40. K. M. O'Hara, M. E. Gehm, S. R. Granade, and J. E. Thomas, "Scaling laws for evaporative cooling in time-dependent optical traps," Phys. Rev. A **64**(5), 051403 (2001).
41. M. Gröbner, P. Weinmann, F. Meinert, K. Lauber, E. Kirilov, and H.-C. Nägerl, "A new quantum gas apparatus for ultracold mixtures of K and Cs and KCs ground-state molecules," J. Mod. Opt. **63**(18), 1829–1839 (2016).
42. N. Gemelke, X. B. Zhang, C.-L. Hung, and C. Chin, "In situ observation of incompressible Mott-insulating domains in ultracold atomic gases," Nature **460**(7258), 995–998 (2009).